

Analysis of structural changes in plasma-deposited fluorinated silicon dioxide films caused by fluorine incorporation using ring-statistics based mechanism

V. Pankov,^{a)} J. C. Alonso, and A. Ortiz

Instituto de Investigaciones en Materiales, Universidad Nacional Autonoma de Mexico, AP 70-360, 04510 Mexico D. F., Mexico

(Received 4 November 1998; accepted for publication 25 March 1999)

Fluorinated silicon dioxide (SiOF) films were prepared by remote plasma enhanced chemical vapor deposition using SiF₄, O₂, H₂, and He reaction gases. Fourier transform infrared spectroscopy studies accompanied by molecular orbital (MO) modeling were used to explain structural changes in SiOF films caused by F incorporation. On the basis of the results of MO modeling, it was shown that F atoms incorporated into the SiOF network only slightly affect the geometry of ring units, the main building blocks of SiOF film network, and cannot cause strong changes in the value of the average Si–O–Si angle, $\langle\theta\rangle$. Ring-statistics-based mechanism is proposed to explain the increase in $\langle\theta\rangle$ in SiOF films with F content. It is supposed that interaction of highly reactive F species from the incoming flux with the growing SiOF network during deposition process induces the preferential conversion of the most strained small-order ring units into those of higher order characterized by larger $\langle\theta\rangle$. As a result, the $\langle\theta\rangle$ in SiOF film increases and film structural homogeneity improves with increasing the F content in the incoming flux. It is assumed that structural changes in SiOF films caused by F incorporation are not the abrupt transition from the ring-built SiOF network to the ring-free chain-like network, but a continuous shift of the ring distribution function towards the large-size high-order rings which causes the increase in $\langle\theta\rangle$ within SiOF network, a reduction in the film density, and an enhancement of the film moisture absorptivity. © 1999 American Institute of Physics. [S0021-8979(99)04613-7]

I. INTRODUCTION

Fluorinated silicon dioxide (SiOF) films have attracted great deal of interest of ultralarge-scale integration circuit manufacturers as a low-dielectric constant insulator material for interlevel metallization. The replacement of oxygen with highly electronegative fluorine has been found to be very effective in the reduction of dielectric constant of SiOF films.^{1–4} However, incorporation of fluorine into the SiO₂ network causes strong structural changes in the SiOF network, observed as blueshift and narrowing of the Si–O–Si asymmetric stretching (s) vibrational peak in the Fourier transform infrared (FTIR) spectra with increasing the fluorine content.^{3–7} Various mechanisms have been proposed to explain the origin of the above structural changes, usually accompanied by reduction in film moisture stability with increasing F content.^{1–3,8,9} It has been supposed elsewhere that the presence of Si–F_n bonds changes Si–O bonding strength,⁶ and induces the transition of the Si–O bonding configuration from the tetrahedral *sp*³ to the planar *sp*² state.³ However, the most common explanation of the blueshift of the above-mentioned peak is that the increased content of Si–F_n bonds within the SiO₂ network affects Si–O–Si units in their vicinity and thereby causes corresponding enlargement in the Si–O–Si bond angle.^{5,7,10}

The microstructure of SiO₂-based amorphous glasses is not the disordered conglomerate of randomly interbonded

Si–O–Si units, but is commonly described using Zachariasen's concept of a continuous random network constructed from reciprocally linked ring structures of Si–O bonds¹¹ where Si–O–Si units are only linkages within the rings structures. These rings may be catalogued statistically according to their order, *n*, equal to the number of Si–O–Si folders in the ring. The experimental data on the ring statistics for plasma-enhanced chemical vapor deposition (PECVD) SiO₂ and SiOF films are very limited. However three and fourfold Si–O ring units have been found recently in the network of low-fluorinated SiOF films.^{5,12,13} Hence it seems to be more reasonable to consider the effect of the fluorine substituent atoms not on the separated Si–O–Si units but on the Si–O–Si units within ring structures.

The recent results of Yoshimaru *et al.*⁵ and Tamura *et al.*^{12,13} evidently show that there is a strong correlation between the content of three and four-fold ring units and F concentration in the SiOF film. It was supposed elsewhere¹² that increased fluorine content during deposition causes the suppression of the three and fourfold rings formation and leads to the transition from the growth of ring-containing SiOF network to that of heavily porous chain-like structure. However theoretical modeling shows that the total ring order distribution in SiO₂-based glass network can embody intermediate range of orders, up to 5, with the main contribution of few orders.^{14,15} Hence it is quite natural to suppose that three and fourfold ring units derived from Raman spectroscopy measurements^{5,12,13} are only a small part in the total

^{a)}Electronic mail: pankov@servidor.unam.mx

ring distribution. Thus it is not clear whether the above transition has the abrupt or continuous character and what in particular is the microstructure of the resulting chain-like network.

In the present work FTIR spectroscopy studies and molecular orbital (MO) modeling are used to explain structural changes in plasma-deposited SiOF films caused by fluorine incorporation. It is demonstrated that an increase in the average Si–O–Si angle, $\langle\theta\rangle$, within SiOF network with increasing fluorine doping level can be explained on the basis of corresponding changes in ring statistics of the SiOF network, taking place during film deposition process.

II. EXPERIMENT

SiOF films were deposited on *n*-type (100) silicon substrates of 200 Ω cm resistivity in a remote plasma enhanced chemical vapor deposition system using $\text{SiF}_4 + \text{O}_2 + \text{H}_2 + \text{He}$ mixture. The reaction chamber used was equipped by an inductively coupled plasma source operating in the high-density plasma regime. The detailed geometry of the reaction chamber is described elsewhere.¹⁵ Flow rates of SiF_4 , O_2 , and H_2 were varied in a wide range from 0.1 to 100 sccm to obtain SiOF films with Si–F_x bond concentration varying from 0 to 8 at. %. The total pressure was of 500 mTorr. Plasma discharge was maintained by rf power at 200 W of 13.56 MHz frequency for all depositions. The substrate temperature was held constant at 175 °C. Film thickness was targeted for 1000 Å to assure the accuracy of FTIR spectroscopy comparative studies.

FTIR absorption spectra were measured by a Nicolet 210 double-beam spectrometer ranging from 400 to 4000 cm^{-1} . The Si–F_x absorption band within the range of 900–1000 cm^{-1} was used to estimate the total atomic concentration of Si–F_x units in SiOF films. The average value of Si–O–Si bonding angle, $\langle\theta\rangle$, was derived from the position of the Si–O–Si stretching (s) vibration peak. The value of $\Delta\theta$, characteristic of film structural homogeneity, was estimated through the analysis of full-width at half-maximum (FWHM) of the same peak. The calculation procedures and the main equations based on the central force model are similar to those presented in Ref. 7.

MO calculations have been performed using GAUSSIAN-94¹⁶ package. Initial geometry was generated using CS Chem3D Pro Version 4.0 software. Depending on the complexity of modeling clusters the stepwise geometry optimization have been carried out using MM2 force field method,¹⁷ a semiempirical Austin Model 1 (AM1) method,¹⁸ or Hartree–Fock method HF/3-21G(*d*) with split valence basis set (3-21G).¹⁹

III. EXPERIMENTAL RESULTS

FTIR spectra of all our as-deposited SiOF films in the entire range of F concentration show three major peaks located at about 1090, 800, and 450 cm^{-1} corresponding to the stretching, bending, and rocking vibrational modes, respectively, of the Si–O–Si bonding²⁰ (see Fig. 1). The presence of other hydrogen-related peaks, e.g., Si–OH and H–OH

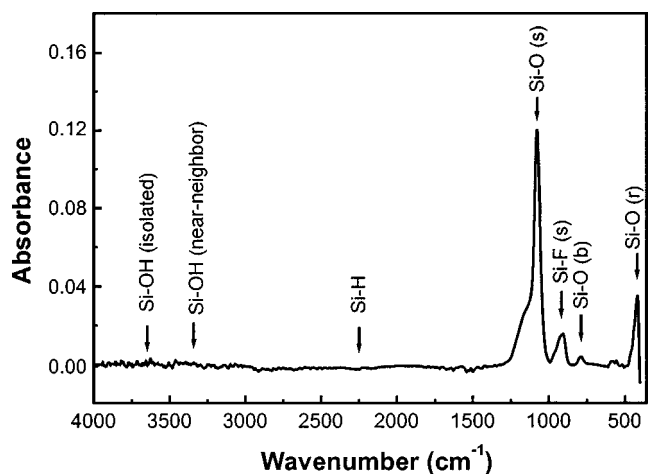


FIG. 1. FTIR spectrum of as-deposited SiOF film prepared with Si–F_x bond concentration of 7.8 at. %. Si–O–Si stretching, bending, and rocking vibrational modes are labeled as (s), (b), and (r), respectively.

(bands ranging at 2800–3750 cm^{-1}),^{20,21} Si–H (2250 and 875 cm^{-1})²² in our as-deposited samples is below FTIR detectable level, $\sim 1\%$.²¹

The main effect of fluorine incorporation is the appearance of the absorption band ranging from about 900 to 1000 cm^{-1} . This band is reportedly attributed to the contribution of stretching vibrations of Si–F_x groups.^{2,5,7} The effect of increasing amounts of fluorine is an incremental shift of Si–O (s) vibration peak position from 1065 cm^{-1} toward higher wave numbers until the value of 1097 cm^{-1} , accompanied by a reduction of the peak FWHM from 81.1 to 45.8 cm^{-1} (see Fig. 2). The peak narrowing is mainly due to the contribution of the low-angular component corresponding to the low-wave number side of Si–O (s) peak, as seen in the figure. Based on the procedure presented elsewhere,⁷ the shift of Si–O (s) vibration peak corresponds to the increase in $\langle\theta\rangle$ from 137.7° to 153.1° as Si–F_x bond content varies from 0 to 8 at. %, as seen in Fig. 3. The values of FWHM are employed to calculate the dispersion of $\langle\theta\rangle$, $\Delta\theta$, using the

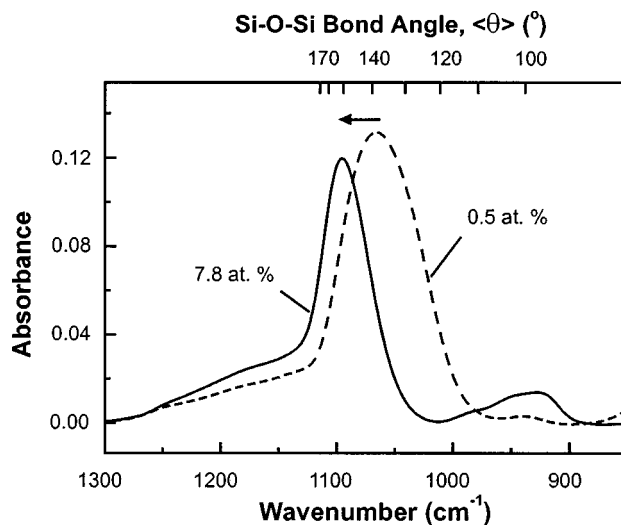


FIG. 2. FTIR spectra in 850–1300 cm^{-1} region of as-deposited SiOF films with Si–F_x bond concentration of 0.5 and 7.8 at. %.

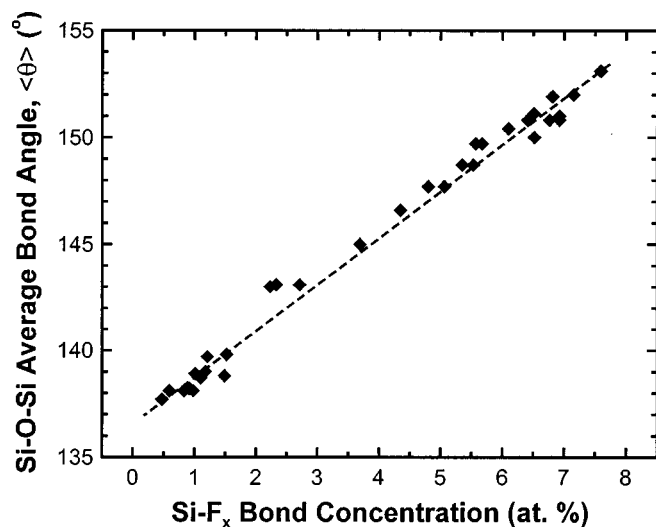


FIG. 3. The average Si–O–Si bond angle vs Si–F_x bond concentration in as-deposited SiOF films.

approach of Han and Aydil.⁷ Figure 4 shows that $\Delta\theta$, an indicator of film structural inhomogeneity, gradually reduces in our as-deposited SiOF films from 32.4° to 28° with increasing F content.

IV. DISCUSSION

A. The effect of F presence on the structure of SiOF network

It has been assumed in numerous studies that the simple presence of F atoms in the network of SiOF films induces strong changes in film microstructure, including the change in Si–O bonding strength,⁶ transition in the Si–O bonding configuration from the tetrahedral sp^3 to the planar sp^2 state,³ the Si–O–Si bond angle enlargement.^{5,7,10}

Ab initio calculations have been performed recently to estimate the change in minimal energy of the optimized geometry for the isolated $(\text{OH})_3\text{Si}-\text{O}-\text{Si}(\text{OH})_3$ molecule if two

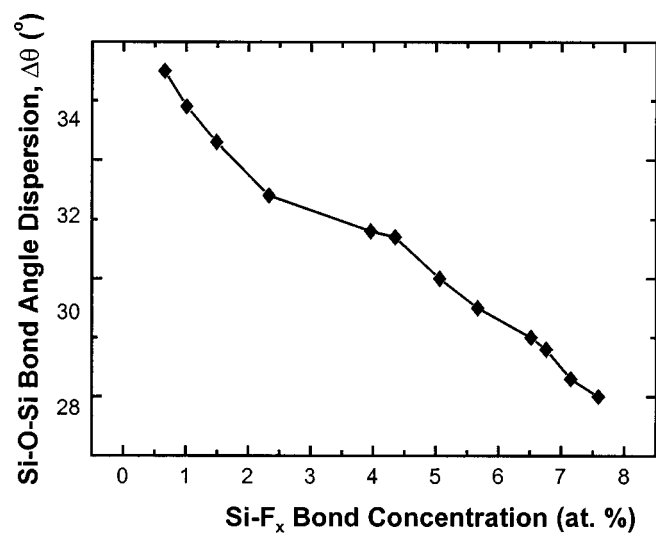


FIG. 4. Si–O–Si bond angle dispersion vs Si–F_x bond concentration in as-deposited SiOF films.

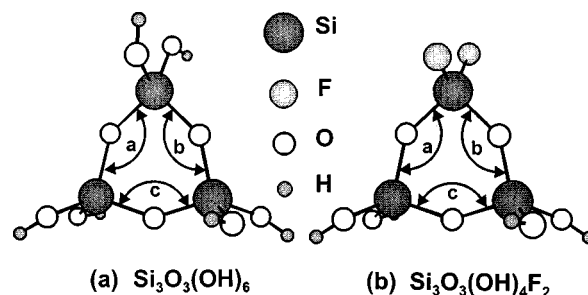


FIG. 5. Threefold siloxane rings modeling clusters of (a) $\text{Si}_3\text{O}_3(\text{OH})_6$ and (b) $\text{Si}_3\text{O}_3(\text{OH})_4\text{F}_2$ used for molecular orbital modeling at the HF/3-21G(d) level of theory. Locations of Si–O–Si angles within ring are labeled with a, b, and c.

F atoms are substituted for the terminal OH groups at the fixed values of Si–O–Si bond angle.¹⁰ However, three and fourfold rings are more real building units of the SiOF film network structure, as it was revealed elsewhere,^{5,12,13} and therefore 2 threefold siloxane ring model clusters, $\text{Si}_3\text{O}_3(\text{OH})_6$ and $\text{Si}_3\text{O}_3(\text{OH})_4\text{F}_2$ (see Fig. 5), were employed in our MO modeling to investigate the effect of Si–F bond presence on the ring geometry. Although FTIR spectra do not show any presence of Si–OH groups in our SiOF films (see Fig. 1), there are several reasons for applying OH termination of Si free valences which are not involved in Si–O–Si bond or cycle formation, as it was done in recent studies.^{8,10} First, SiOF films obtained by PECVD usually contain relatively low concentration of Si and O dangling bonds to be considered as an open-shell system, therefore a termination of both Si and O free valences is required for thorough MO modeling. Oxygen termination of Si free valencies that are not involved in the ring formation allows us to take into consideration interactions between substituting oxygen atoms, which are known to strongly affect the Si–O–Si bond angle, as it was shown elsewhere.¹⁰ Free valencies of oxygen also require their termination, that can be done using the smallest and moderately electronegative hydrogen atom, which is assumed to produce a minimal effect on the ring geometry compared with other elements of the periodic table. Taking into account all aforementioned, siloxane ring model clusters were thought to be sufficiently appropriate for studying the effect of F presence on the ring geometry. The presence of two fluorine atoms within threefold ring unit shown in Fig. 5, b approximately corresponds to 25 at. % of F in the SiOF network built from the above ring units. The placement of two substituent F atoms at the same Si atom [see Fig. 5, b] is supposed to cause the maximal deformation effect on the ring geometry. Preliminary geometry optimization was conducted by AM1 method. Final *ab initio* calculations were performed at HF/3-21G(d) theory level.

The results of the above MO modeling are presented in Table I and clearly show only minute distortion in θ within a threefold ring unit at almost an unchangeable value of $\langle\theta\rangle$. These results are coincident with *ab initio* calculations of Lucovsky and Yang¹⁰ who have observed only a minute change in the energy of $\text{H}_6\text{Si}_2\text{O}_7$ molecule if two F atoms are substituted for the terminal OH groups. A possible explana-

TABLE I. Si–O–Si bond angles in $\text{Si}_3\text{O}_3(\text{OH})_6$ and $\text{Si}_3\text{O}_3(\text{OH})_4\text{F}_2$ ring modeling clusters after HF/3-21G(d)//AM1 geometry optimization. Cluster geometry and locations, a, b, and c angles are shown in Fig. 5.

Modeling cluster	Si–O–Si bond angles within ring ($^\circ$)			Average value ($^\circ$)
	a	b	c	
$\text{Si}_3\text{O}_3(\text{OH})_6$	136.5309	136.5334	135.931	135.9984
$\text{Si}_3\text{O}_3(\text{OH})_4\text{F}_2$	134.5892	134.5697	138.8777	136.0122

tion of these findings is that small three and fourfold rings have a great deal of small-angle strain, similar to small (three and four membered) polymer rings, where small-angle strain drastically reduces with increasing ring order,²³ and therefore their geometry is very stable to the effect of F-terminating atom. On this basis, Si–O ring units of higher orders should be less strained and thereby more sensitive to the F presence. To check this assumption comparative analysis of the geometry change in eight-fold ring units if two F atoms were substituted for the terminal OH groups at the same Si atom, was performed on the AM1 theory level. The results are presented in the Table II and evidently show that even in this case the changes in $\langle\theta\rangle$ are very small, by about 0.25° . Hence, other mechanisms are surmised to contribute to the changes of $\langle\theta\rangle$ in the SiOF films.

B. The role of F during SiOF film deposition

We suppose that not the effect of F on its environment within the network of as-deposited SiOF film, but the presence of F in the incoming flux as F radicals, ions, F_2 , or as a part of precursors and by-products of plasma-chemical reactions during film deposition results in radical changes in the structure of the growing SiOF network.

It was reported in numerous studies that during SiOF film deposition a certain fraction of extremely reactive F species characterized by high etching ability, usually present in the incoming flux, etches the growing SiOF network, presumably through the substitution reaction with bridging oxygen.^{6,7,9,10} Taking into account the presence of highly strained three and fourfolded ring units in SiOF network, it is likely that the most strained Si–O bonds of low-order ring units are broken first. The result of this attack should be the conversion of low-order rings to higher order ones and the formation Si–F terminating bonds. The above mechanism is confirmed by the decrease of the intensity of Raman peaks assigned to three and fourfold rings with increasing F content in SiOF film, as it was observed elsewhere.^{5,12,13}

Considering the attack of F on the SiOF network, it should be taken into account that all the ring units are reciprocally bonded and breaking of any bridging oxygen bond

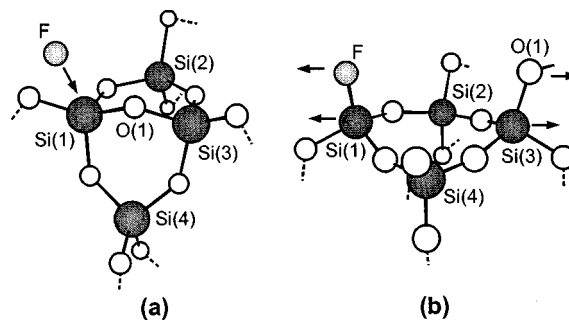


FIG. 6. Mechanism of F incorporation through the oxygen substitution mechanism. (a) Two adjacent three-fold ring units under the attack of F radical to the common Si atom. (b) Result of the attack: conversion of two three-fold rings into one four-fold ring unit; appearance of Si–F bond and O dangling bond and their reciprocal removal. Bonding of Si atoms to the surrounding SiOF network through the O atoms is marked by dashed lines.

results in joining two adjacent n_1 - and n_2 -folded rings with the formation of a new ring of higher order, equal to $(n_1 + n_2 - 2)$. Figure 6 demonstrates the attack of F radical on the bridging Si–O unit belonging to two adjacent three-fold rings. The results of this attack are: (a) Si(1)–O(1) bond breaking, (b) Si(1)–F bond formation, and (c) appearance of O(1) dangling bond. Later, unpaired localized electron at O(1) atom can be either bonded to another silicon atom (O–F bonding was found to occur in plasma-deposited SiOF films at oxygen-rich deposition conditions only⁷) or involved in stepwise reactions with incoming precursors and particles arriving from the plasma region. It is also assumed that during film deposition at low substrate temperature F and O(1) atoms cannot achieve the energetically shallowest state due to the steric hindrance effect. Therefore, it is very likely that O(1) atom is weakly bonded and therefore can also be substituted by another F radical resulting in the formation of near-neighboring F termination.

C. Ring-statistics based mechanism of SiOF film structural changes

In the previous section it has been shown that Si–O bonds of low-order ring units are the most strained and hence should be broken first through the attack of F species to the SiOF network causing changes in ring statistics toward higher orders. It is quite natural to expect that the above changes in ring statistics can result in corresponding changes in $\langle\theta\rangle$ which can cause the blueshift of the Si–O (s) peak, shown in Fig. 2.

Galeener has reported that the value of the inner θ_n within planar ring of order n can be derived from the following equation where φ is the O–Si–O angle found to be narrowly distributed around 109.5° :²⁴

TABLE II. Si–O–Si bond angles in $\text{Si}_8\text{O}_8(\text{OH})_{16}$ and $\text{Si}_8\text{O}_8(\text{OH})_{14}\text{F}_2$ ring modeling clusters after AM1 geometry optimization.

Modeling cluster	Si–O–Si bond angles within ring ($^\circ$)								Average value ($^\circ$)
	a	b	c	d	e	f	g	h	
$\text{Si}_8\text{O}_8(\text{OH})_{16}$	170.130	159.085	164.304	167.077	169.716	157.322	163.923	170.822	165.297
$\text{Si}_8\text{O}_8(\text{OH})_{14}\text{F}_2$	169.898	158.966	164.187	166.306	168.987	156.904	163.989	171.191	165.053

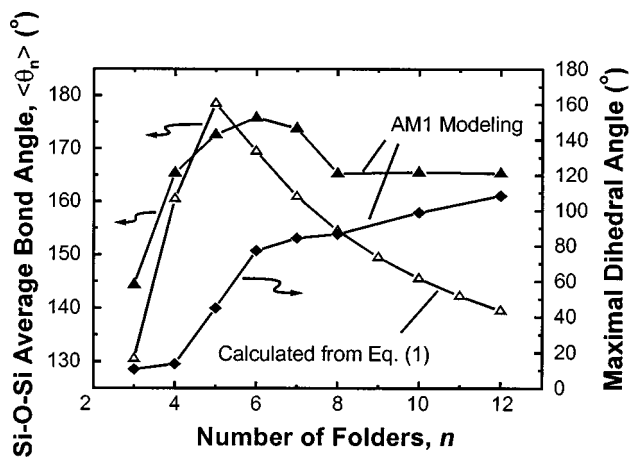


FIG. 7. Si–O–Si bond angle within ring calculated using Eq. (1) for planar rings, by molecular orbital modeling at the AM1 level of theory (average value) vs number of folders within ring, and maximal value of dihedral angle within ring as a function of the number of ring folders, characteristics of ring deplanarization ability.

$$\theta_n = 360(1 - n^{-1}) - \varphi. \quad (1)$$

Hence, θ_n is of 130.5° for threefold ring, 160.5° for fourfold ring, and 178.5° for fivefold ring. Following Eq. (1) planar n -order rings with n equal 6 and more have $\theta_n > 180^\circ$ with respect to the inner ring volume. FTIR spectroscopy gives the angle between Si–O bonds within Si–O–Si units therefore $\theta_n > 180^\circ$ are recalculated as $(360^\circ - \theta_n)$ and shown in Fig. 7.

Figure 7 shows that for high order rings θ_n should decrease opposite to our experimental results. However Eq. (1) does not take into account deplanarization effects playing a considerable role in ring geometry when a number of folders exceeds the value of 4, as it was reported elsewhere.²⁴ To take into account the effect of ring deplanarization, MO modeling studies based on the AM1 level of theory have been performed for ring units with a number of folders, n , ranging from 3 to 12.

Figure 7 demonstrates the results of MO modeling where $\langle \theta_n \rangle$ as a function of ring order is presented. The value of $\langle \theta_n \rangle$ sharply increases initially with increased number of folders, and then a slight reduction is followed by $\langle \theta_n \rangle$ saturation at about 165° , when n exceeds 7. To explain the above trend it is worth mentioning the results of the recent *ab initio* modeling using $(\text{OH})_3\text{Si}-\text{O}-\text{Si}(\text{OH})_3$ molecule as a modeling cluster.¹⁰ It has been found *ibid.* that the optimized geometry of this molecule is characterized by an unusual value of Si–O–Si angle equal to 180° . This is probably due to the strong interaction between substituent oxygen atoms. It is assumed that at $n > 7$ the flexibility of ring is high enough to provide a ring geometry which neglects the interaction between remote substituents. Hence only interactions between nearest substituent oxygen atoms determine ring geometry resulting in almost similar $\langle \theta_n \rangle$ when n exceeds 7. This is coincident with a strong deplanarization trend observed for the rings with n above 6. To estimate the degree of deplanarization, the values of dihedral angles between two planes defined by $A(1)-A(2)-A(3)$ and $A(2)-A(3)-(4)$, where $A(1)...A(4)$ are any four consecutive atoms of the ring,

where measured. It was found that the value of the maximal dihedral angle within rings starts to saturate beginning from $n=6$, which is coincident with starting in $\langle \theta_n \rangle$ reduction, as seen in Fig. 7. Thus, it can be concluded that an increased flexibility of rings with n above 6 results in strong deplanarization of the ring geometry, which causes an effective relaxation of the small-angle strain, typical for low-order ring units. As a consequence, the value of $\langle \theta_n \rangle$ starts to decrease beginning from $n=6$, and saturates at $n=8$.

Based on the results of MO modeling it is assumed that the main mechanism contributing to the drastic increase in $\langle \theta \rangle$ with F content in SiOF films is a ring-statistics based mechanism. Low-temperature deposition results in low surface mobility of the precursors making them occupy energetically unfavorable sites on the film surface. The presence of charged and high-energetic particles in the incoming flux, typical for PECVD processes, generates the additional nucleation centers. Hence, it may well be that the main building blocks of pure PECVDSiO₂ films are heavily strained low-order ring units resulting in low $\langle \theta \rangle$ in as-deposited films ranging from 136° to 144° .^{7,25} The presence of highly reactive F species in the incoming flux activates the conversion of the most strained low-order ring units with small $\langle \theta_n \rangle$ into those of higher order characterized by bigger $\langle \theta_n \rangle$ causing strong blueshift and narrowing of the Si–O (s) peak, mainly due to the reducing contribution of the low-wave number component corresponding to the small-angular Si–O–Si groups, as seen in Fig. 2. The above changes in ring statistics with increasing F content are assumed to be responsible for the reduction in film density^{7,26} and increase of water absorptivity of SiOF film,^{2,3} as the fluorine doping level increases. It is surmized that both the bigger size of high-order rings and multiple F termination, which reduces the total interbonding of the SiOF network, cause an additional microvoids formation, as it was supposed elsewhere.^{3,12}

Thus, it can be concluded that increased content of reactive F species in the incoming flux results not only in the SiOF film with increased fluorine content, but also in changing ring statistics of the SiOF network towards higher order rings. The consequence of these structural changes is almost linear increasing $\langle \theta_n \rangle$ in the range of Si–F_x bond concentrations from 0 to 8 at. %, as seen in Fig. 3. Subsequent increase in fluorine content should lead to the slight reduction in $\langle \theta_n \rangle$ with following saturation, as show the results of AM1 modeling (see Fig. 7). Indeed, Nakasaki *et al.*⁸ observed the saturation in the Si–O (s) peak blueshift at the fluorine content of around 12 at. % in SiOF films. Moreover, Han and Aydil also found the saturation in Si–O–Si bond angle raising at the Si–F_x bond concentrations of about 12 at. %.⁷ The maximal content of Si–F_x bonds in our films was of 8 at. % which is assumed to be below the saturation region, resulting in an almost linear relationship between $\langle \theta \rangle$ and Si–F_x bond content (see Fig. 3). The lack of the slight reduction trend predicted by MO calculations (see Fig. 7), but not observed elsewhere^{7,8} can be due to both partial bonding of surface ring units and low deposition temperatures, which reduces the flexibility of these rings and causes a certain discrepancy between the results of MO modeling and experiments.

D. Film structural homogeneity versus F content

The changes in $\Delta\theta$ in our films versus F content shown in Fig. 4 cannot be explained based on the effect of F on its environment within SiOF network of as-deposited SiOF film. It was reported elsewhere⁸ that about 12 at. % incorporated F can affect about 50% of Si–O–Si linkages, while other bonds remain unaffected. Hence, $\Delta\theta$ in SiOF films should initially increase with F content, then reduce when F starts to affect the majority of Si–O–Si linkages. Actually, Fig. 4 shows only monotonous reduction in $\Delta\theta$ in as-deposited SiOF film with increasing F content. It seems that structural homogeneity of the film should improve with increasing F content in the incoming flux because of the effective removal of the extreme (i.e., the most strained) bonding units from the growing SiOF network, similar to the experimentally observed trend. It is also probable that low-order ring conversion can produce Si–O–Si linkages with very large θ or weakly bonded. It is likely that all the extreme bonding groups are removed from the growing SiOF network because of the selective etching effect of F species during film growth causing the improvement of film structural homogeneity.

V. CONCLUSIONS

Based on the results of FTIR spectroscopy studies accompanied by molecular orbital modeling studies it is shown that F atoms incorporated into the SiOF network only slightly affects the geometry of ring units, the main building blocks of SiOF film network, and cannot cause strong changes in the value of $\langle\theta\rangle$ in the SiOF film.

Ring-statistics-based mechanism is proposed to explain the increase in $\langle\theta\rangle$ in SiOF films with F content. It is supposed that interaction of highly reactive F species from the incoming flux with the growing SiOF network during the deposition process induces the preferential conversion of the most strained small-order ring units into those of higher order. As a result, the $\langle\theta\rangle$ in SiOF film increases and film structural homogeneity incrementally improves with increasing F content in the incoming flux.

It is assumed that structural changes in SiOF films caused by F incorporation are not the abrupt transition from the SiOF network built from three- and four-folded ring units to the ring-free chain-like network, as it was assumed elsewhere,¹² but rather a continuous shift of the ring distribution function towards high-order rings resulting in corresponding changes in $\langle\theta\rangle$ within SiOF network, film density, and moisture reactivity. The network of high-fluorinated SiOF films should consist of high-order ring units. Due to the big size of high-order rings and multiple F termination which reduces a total interbonding of the SiOF network, high-

fluorinated SiOF films should have reduced density, increased water absorptivity, and should be more susceptible to the attack of water.

This work was partially supported by DGAPA under Project No. IN100997 and CONACyT under the Project No. 26423-A. The authors would like to thank Dr. S. Fomine for his valuable discussions and help with the molecular orbital modeling.

- ¹S. W. Lim, Y. Shimogaki, Y. Nakano, K. Tada, and H. Komiyama, *Jpn. J. Appl. Phys.*, Part 1 **35**, 1468 (1996).
- ²M. Yoshimaru, S. Koizumi, and K. Shimokawa, *J. Vac. Sci. Technol. A* **15**, 2915 (1997).
- ³M. K. Bhan, J. Huang, and D. Cheung, *Thin Solid Films* **308/309**, 507 (1997).
- ⁴W. T. Tseng, Y. T. Hsieh, C. F. Lin, M. S. Tsai, and M. S. Feng, *J. Electrochem. Soc.* **144**, 1100 (1997).
- ⁵M. Yoshimaru, S. Koizumi, and K. Shimokawa, *J. Vac. Sci. Technol. A* **15**, 2908 (1997).
- ⁶T. Usami, K. Shimokawa, and M. Yoshimaru, *Jpn. J. Appl. Phys.*, Part 1 **33**, 408 (1994).
- ⁷S. M. Han and E. S. Aydil, *J. Vac. Sci. Technol. A* **15**, 2893 (1997).
- ⁸Y. Nakasaki, H. Miyajima, R. Katsumata, and N. Hayasaka, *Jpn. J. Appl. Phys.*, Part 1 **36**, 5259 (1997).
- ⁹M. J. Shapiro, S. V. Nguyen, T. Matsuda, and D. Dobuzinsky, *Thin Solid Films* **270**, 503 (1995).
- ¹⁰G. Lucovsky and H. Yang, *Jpn. J. Appl. Phys.*, Part 1 **36**, 1368 (1997).
- ¹¹W. H. Zachariasen, *J. Am. Chem. Soc.* **54**, 3841 (1932).
- ¹²T. Tamura, J. Sakai, M. Satoh, Y. Inoue, and H. Yoshitaka, *Jpn. J. Appl. Phys.*, Part 1 **36**, 1627 (1997).
- ¹³T. Tamura, J. Sakai, Y. Inoue, M. Satoh, and H. Yoshitaka, *Jpn. J. Appl. Phys.*, Part 1 **37**, 2411 (1998).
- ¹⁴A. C. Wright, G. Etherington, J. A. E. Desa, R. N. Sinclair, G. A. N. Connel, and J. C. Mikkelsen, *J. Non-Cryst. Solids* **49**, 63 (1982).
- ¹⁵V. Pankov, J. C. Alonso, and A. Ortiz, *Jpn. J. Appl. Phys.*, Part 1 **37**, 6135 (1998).
- ¹⁶M. J. Frisch, G. W. Trucks, H. B. Schlegel, P. M. W. Gill, B. G. Johnson, M. A. Robb, J. R. Cheeseman, T. Keith, G. A. Petersson, J. A. Montgomery, K. Raghavachari, M. A. Al-Laham, V. G. Zakrzewski, J. V. Ortiz, J. B. Foresman, J. Cioslowski, B. B. Stefanov, A. Nanayakkara, M. Challacombe, C. Y. Peng, P. Y. Ayala, W. Chen, M. W. Wong, J. L. Andres, E. S. Replogle, R. Gomperts, R. L. Martin, D. J. Fox, J. S. Binkley, D. J. Defrees, J. Baker, J. P. Stewart, M. Head-Gordon, C. Gonzalez, and J. A. Pople, *GAUSSIAN 94* (Gaussian, Pittsburgh, PA, 1995), Revision E.3.
- ¹⁷M. Mansfield and L. Klushin, *Macromolecular* **26**, 4262 (1993).
- ¹⁸J. J. P. Stewart, *J. Comput. Chem.* **10**, 209 (1989).
- ¹⁹J. Foresman and A. Frish, *Exploring Chemistry with Electronic Structure Methods* (Gaussian, Pittsburgh, PA, 1996).
- ²⁰W. A. Pliskin, *J. Vac. Sci. Technol.* **14**, 1064 (1977).
- ²¹J. A. Theil, D. V. Tsu, M. W. Watkins, S. S. Kim, and G. Lucovsky, *J. Vac. Sci. Technol. A* **8**, 1374 (1990).
- ²²D. V. Tsu, B. N. Davidson, and G. Lucovsky, *Phys. Rev. B* **40**, 1795 (1989).
- ²³J. March, *Advanced Organic Chemistry* (Wiley, New York, 1985), pp. 130–136.
- ²⁴F. L. Galeener, *J. Non-Cryst. Solids* **49**, 53 (1982).
- ²⁵A. Brunet-Bruneau, J. Rivory, B. Rafin, J. Y. Robic, and P. Chaton, *J. Appl. Phys.* **82**, 1330 (1997).
- ²⁶H. Kudo, R. Shinohara, S. Takeishi, N. Awaji, and M. Yamada, *Jpn. J. Appl. Phys.*, Part 1 **35**, 1583 (1996).